Self-Organization of Sorted Patterned Ground

M. A. Kessler*† and B. T. Werner

Striking circular, labyrinthine, polygonal, and striped patterns of stones and soil self-organize in many polar and high alpine environments. These forms emerge because freeze-thaw cycles drive an interplay between two feedback mechanisms. First, formation of ice lenses in freezing soil sorts stones and soil by displacing soil toward soil-rich domains and stones toward stone-rich domains. Second, stones are transported along the axis of elongate stone domains, which are squeezed and confined as freezing soil domains expand. In a numerical model implementing these feedbacks, circles, labyrinths, and islands form when sorting dominates; polygonal networks form when stone domain squeezing and confinement dominate; and stripes form as hillslope gradient is increased.

Patterns delineated by distinct stone and soil (fine-grained) domains visible at the ground surface are formed by cyclic freezing and thawing of decimeter- to meter-thick soil layers in polar and high alpine environments. The observed range of sorted patterned ground includes sorted circles, labyrinthine stone and soil networks, stone islands, sorted polygons, and sorted stripes on hillslopes (Fig. 1). These quintessential forms constitute one of the most striking suites of geomorphic patterns. The diversity of sorted patterned ground has been attributed to a multiplicity of formation mechanisms (*1*). The underlying processes include particle sorting (*2, 3*), freezing and thawing (*2, 4, 5*), deformation of frozen soil (*6*), and soil creep (*7*), but the range of forms has not been captured in a single model (*8–11*).

Patterns in a broad range of environments have been hypothesized to form by self-organization [e.g., (*12–17*)], whereby nonlinear, dissipative interactions among the small- and fast-scale constituents of a system give rise to order at larger spatial and longer temporal scales (*18*). Because transport in the active layer (the soil layer experiencing annual or diurnal freezing and thawing) is highly nonlinear and dissipative, self-organization is a candidate for the general mechanism underlying sorted patterned ground (*10–12*). In this case, a smooth change in controlling parameters might lead to an abrupt shift in the type of sorted patterned ground without a change in processes causing the pattern. We have developed a numerical model within which sorted patterned ground self-organizes, with transitions between patterns controlled by the relative magnitude of two feedback mechanisms plus hillslope gradient.

Complex Systems Laboratory, Cecil and Ida Green Institute of Geophysics and Planetary Physics, University of California, San Diego, La Jolla, CA 92093, USA.

*Present address: Earth Sciences Department, University of California, Santa Cruz, CA 95064, USA.
†To whom correspondence should be addressed. E-mail: mkessler@es.ucsc.edu

The first feedback (Fig. 2), between stone-soil interface morphology and transport of stones and soil by frost heave, acts to laterally sort the active layer by moving stones toward areas of high stone concentration and soil toward areas of high soil concentration. Given a layer of stones overlying fine-grained soil (formed by deposition or vertical sorting), a laterally uniform stone-soil interface is unstable to perturbations because of frost heave near the interface. A freezing front (0° isotherm) descending from the ground surface mimics the morphology of the stone-soil interface because it descends faster in overlying stone regions (which are dry) than in fine-grained soils [which retain substantial water and must freeze as well as be cooled (*19–21*)]. Consequently, where the interface is inclined, frost heave (which acts normal to the freezing front) pushes soil down and toward soil-rich regions and pushes stones up and toward stone-rich regions, eventually giving rise to distinct stone and soil domains (*11, 22*).

The second feedback, between stone domain morphology and stone transport, stabilizes and promotes elongation of linear stone domains by transporting stones along their axes. Laterally directed frost heave near the stone-soil interface squeezes the stone domain (*23*), thereby elevating its surface by an amount proportional to lateral frost heave. Resulting along-axis gradients in uplift drive stone transport along the stone domain if stones are laterally confined within stone domains. Such confinement is promoted by low surface relief across stone domains, which results when rapid freezing of stone domains causes uniform lateral frost heave with depth in surrounding soils (*24*). Squeezing and confinement stabilize the vertical thickness of stone domains, because uplift increases with thickness, causing stones to avalanche from regions of high to low thickness. Similarly, squeezing and confinement stabilize the width of stone domains because wider sections, which are deeper and more easily deformed (*25*), experience greater uplift than do narrower sections. Squeezing and confinement also elongate stone domains because uplift promotes avalanching of stones toward and off narrow and shallow ends.

In a numerical model implementing these feedbacks (*26*), stones move in two dimensions representing an active layer in plan view (*27*). The effects of soil domains on stones are calculated from the current configuration of stones. Beginning with a random configuration, the two feedback mechanisms drive incremen-

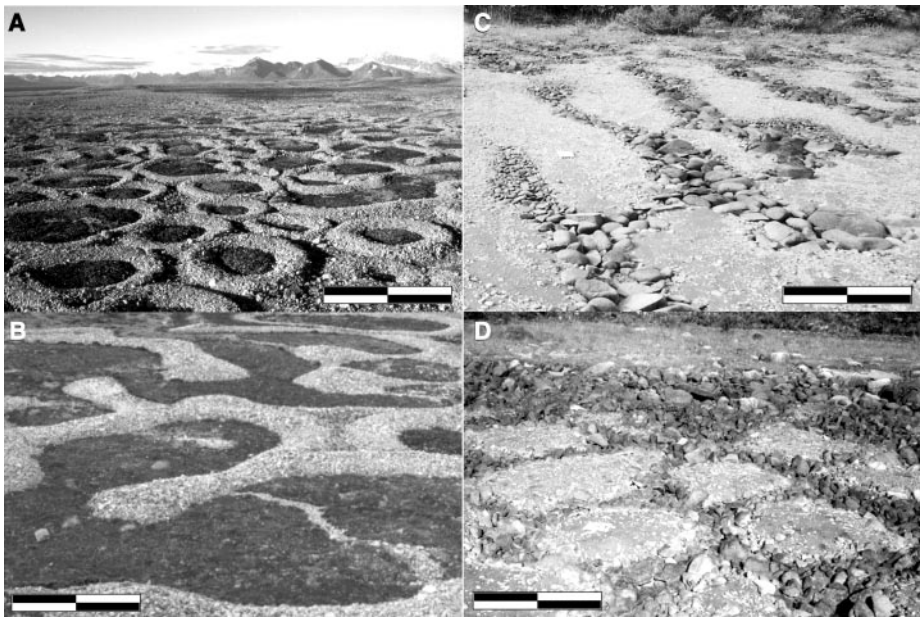

Fig. 1. Forms of sorted patterned ground (scale bars apply to foreground): (**A**) sorted circles (full scale bar ~2 m) and (**B**) sorted labyrinths (full scale bar ~1 m), Kvadehuksletta, Spitsbergen; (**C**) sorted stripes (full scale bar ~1 m), Tangle Lakes region, Alaska; and (**D**) sorted polygons (full scale bar ~1.0 m), Denali Highway, Alaska.

tal stone displacements over repeated iterations, each of which represents a freeze-thaw cycle. Additionally, during each iteration, surface stones are displaced downslope a distance proportional to the hillslope gradient.

Lateral sorting is abstracted by first calculating a surface, H, that decreases with local stone concentration [averaged over a radius D_{ls} (*28*) and weighted by inverse distance], which represents a smoothed version of the stone-soil and air-soil interfaces. Then stones are moved a distance $\delta\mathbf{x}_{ls}$ downslope (toward regions of high stone concentration) proportional to the local gradient of this surface [$\delta\mathbf{x}_{ls} = K_{ls} \nabla H$, where K_{ls} is a diffusion constant (*29*) determining the rate of stone motion]. Far from a stone domain, these displacements represent transport by surface creep; close to a stone domain, they represent the combined effects of surface creep and sorting caused by frost heave at freezing fronts inclined to the stone-soil interface. This abstraction simulates the positive feedback of lateral sorting because areas of high stone concentration generate dips in the surface that attract more stones.

Within stone domains, motion by lateral squeezing and confinement is abstracted as diffusion of stones biased parallel to the axis of the stone domain: $\delta\mathbf{x}_{sq} = |K_{sq} \nabla U|\hat{\boldsymbol{u}}$, where U is the surface uplift owing to lateral squeezing of the stone domain (*26*) and K_{sq} is a diffusion constant (*29*) determining the rate of downslope stone transport. The direction of transport, $\hat{\boldsymbol{u}}$, is the average of a unit vector pointing along the axis of the stone domain (determined over a distance D_{sq} and weighted by a constant factor C_{sq}) and a randomly oriented unit vector (weighted by the factor $1 - C_{sq}$). The length scale D_{sq} corresponds to the distance over which the direction of lateral frost heave varies, as controlled by heat conduction and the thickness of the frozen layer (*30*). The nondimensional weighting C_{sq} (ranging from 0 to 1) encapsulates the degree of confinement of stones to the stone domain; increasing C_{sq} increases the along-axis component of stone diffusion and decreases the radially symmetric component. Increasing K_{sq} represents increasing lateral squeezing and uplift, which increases the along-axis and radially symmetric components of stone diffusion. Changing the along-axis component of stone diffusion independent of the radially symmetric component can be accomplished if K_{sq} and C_{sq} are varied simultaneously, keeping $K_{sq}(1 - C_{sq})$ constant.

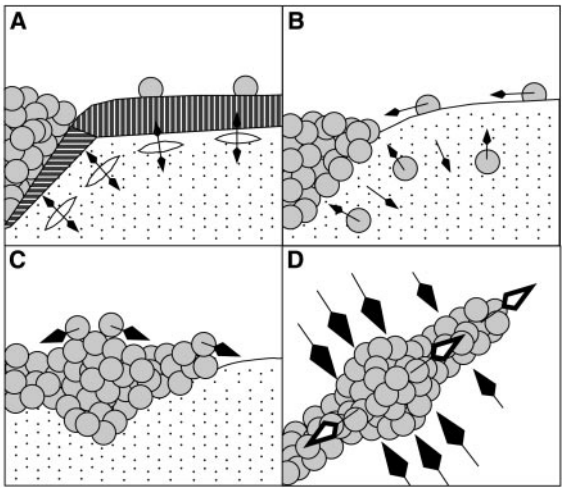

Fig. 2. Feedback mechanisms for sorted patterned ground: lateral sorting (A and B) and lateral squeezing and confinement (A, C, and D). (**A**) Frost heave expands soil perpendicular to the freezing front (cross section). Horizontal lines indicate zone of lateral frost heave near the stone-soil interface; vertical lines indicate zone of vertical frost heave near the ground surface. (**B**) Surface stones creep toward stone domains, subsurface soil is driven toward the interior of the soil domain, and stones are pushed toward stone domains by frost heave near the stone-soil interface (cross section) (*11*). (**C**) Stones avalanche away from regions where stone domains are thicker, which experience greater uplift by lateral squeezing (vertical section along the stone domain axis). (**D**) Regions where stone domains are wider experience greater uplift owing to lateral squeezing (plan view); stone motion (open arrows) is away from wider areas and parallel to the stone domain axis.

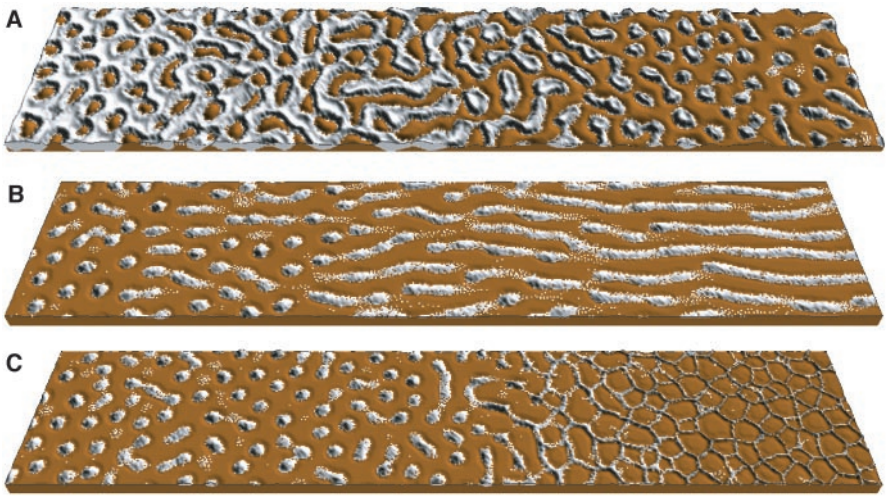

Fig. 3. Sorted patterned ground model simulations showing pattern transitions with varying parameters (three-dimensional perspective view with gray stone domains and brown soil domains). (**A**) Stone concentration decreases left to right from 1400 to 100 stones/m^2; lateral confinement $C_{sq} = 0.0$. (**B**) Hillslope gradient increases left to right from 0° to 30°; $C_{sq} = 0.0$, 100 stones/m^2. (**C**) C_{sq} increases left to right from 0.0 to 1.0, 100 stones/m^2. Simulation size = 50 × 10 m, cell width = 0.1 m, lateral sorting length scale $D_{ls} = 0.5$ m, lateral sorting diffusion constant $K_{ls} = 0.005$ m^2/cycle, lateral squeezing length scale $D_{sq} = 0.2$ m, lateral squeezing constant $K_{sq}dw = 0.002$ m^3/cycle (where dw is the amount of squeezing), maximum depth of stone domains $H_{max} = 20$ stones, 500 iterations.

Physically, the transition from islands to polygons can be attributed to decreased soil compressibility and rapid freezing in stone domains with large air-cooled pores (large stones). Less compressible soil reduces the lateral sorting mechanism that causes instabilities in the depth of stone domains. Rapid freezing increases lateral frost heave at depth, which increases squeezing and reduces the surface relief across stone domains (*24*), thereby increasing confinement.

As the mean concentration of stones, the hillslope gradient, and the degree of lateral confinement were varied in our model, sorted circles, labyrinths, islands, stripes, and polygons emerged (Fig. 3). Without lateral confinement ($C_{sq} = 0$) and as stone concentration was decreased, sorted circles transitioned to labyrinths at ~1000 stones/m^2 and then to stone islands at ~700 stones/m^2 (Fig. 3A), because isolated stone domains coalesce when separated by a distance less than the length scale associated with subsurface soil motion by frost heave, D_{ls}. With stone concentration fixed at ~100 stones/m^2 and increasing hillslope gradient, stone islands transitioned to downslope stripes at ~10° (Fig. 3B). This transition is determined by the magnitude of downslope transport away from a stone domain versus transport toward the stone domain by lateral sorting processes, and consequently it occurs at increasing hillslope gradient as lateral sorting into stone and soil domains progresses. Stone islands transitioned to sorted polygons with increasing lateral confinement (C_{sq}, Fig. 3C) or along-axis transport (K_{sq}). For $C_{sq} > \sim 0.6$, the outward transport of stones owing to lateral squeezing exceeded the inward transport of stones by lateral sorting processes, and stone islands were drawn out into the linear stone domains of sorted polygons.

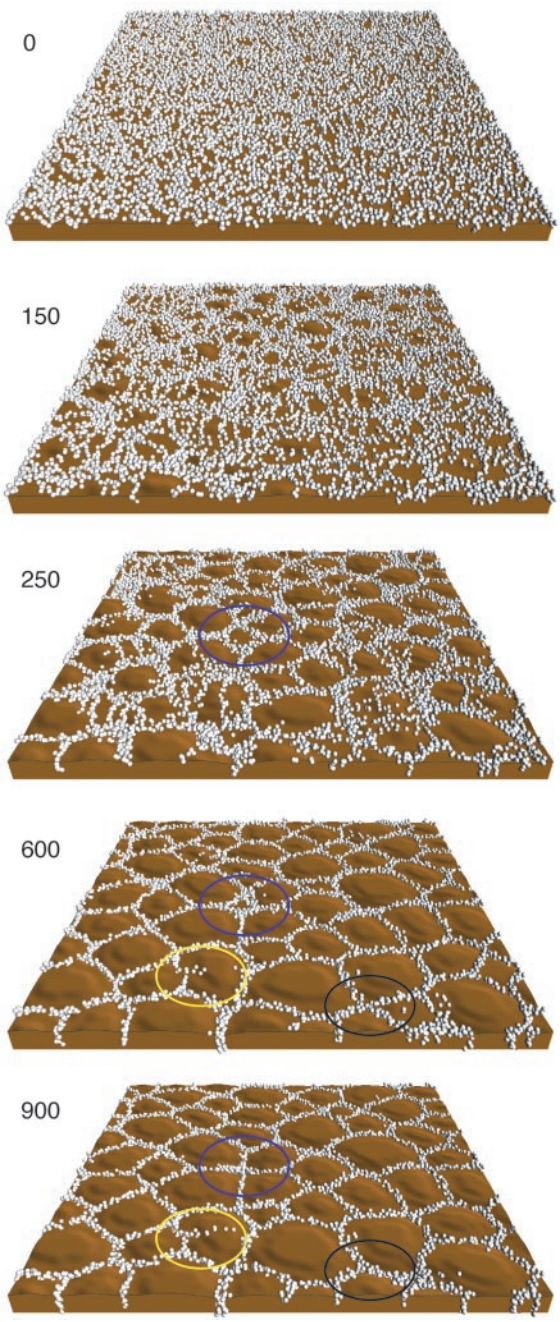

Fig. 4. Development of sorted polygons from a random initial configuration. Blue ovals indicate a small polygon evolving to an intersection. Black ovals indicate a transition from a four-way to a three-way intersection through the shrinking of a neighboring soil domain. Yellow ovals indicate an unstable perturbation on a stone domain extending across a soil domain. Numbers indicate the iteration pictured. Simulation size = 10 × 10 m, 10,000 stones, cell width = 0.1 m, D_{ls} = 0.5 m, K_{ls} = 0.005 m^2/cycle, D_{sq} = 0.2 m, $K_{sq}dw$ = 0.002 m^3/cycle, C_{sq} = 1.0, H_{max} = 10 stones.

Sorted polygons (Fig. 4) experience richer dynamics than other patterns because they result from an interplay between the two feedback mechanisms. Three-way intersections became equiangular in our model because frost heave–induced squeezing was reduced and less focused in the soil domain bordered by the stone domains forming the smallest intersection angle. Therefore, stones preferentially avalanched toward the smallest intersection angle, causing the intersection to migrate in this direction, thereby increasing the smallest intersection angle at the expense of the other two. This mechanism also causes four-way intersections to be unstable. At the intersection, lateral squeezing from frost heave in the soil domains enclosed by the two (generally opposing) larger intersection angles is greater than that in the other two soil domains; therefore, stones are squeezed between the larger soil domains and consequently avalanche toward the two soil domains enclosed by the smaller intersection angles. This divergent stone avalanching from the intersection elongates the four-way intersection into a linear stone domain with a three-way intersection at each end.

The initial spacing of sorted polygons generally was two to three times the radius over which stone concentration was calculated, D_{ls}. The mean polygon size increased by elimination of polygons with fewer sides than the polygons that surrounded them. The tendency of intersections to move in the direction of the smallest intersection angle causes polygons with fewer sides (and therefore smaller intersection angles) to shrink to four-way or five-way intersections that then transition to three-way intersections (Fig. 4). Similar transitions in soap bubbles and magnetic fluid froths have been reported (*31, 32*).

Table 1. Statistical comparisons of polygon area and angle distributions in Fig. 5. Values are probabilities of correctly rejecting the null hypothesis that a given pair of distributions does not share the same parent distribution, calculated using the Kolmogorov-Smirnov test.

Distributions	Angle	Area
Model-model	0.7 ± 0.2	0.8 ± 0.2
East-model	0.6 ± 0.1	0.82 ± 0.05
West-model	0.5 ± 0.1	0.4 ± 0.2
East-west	0.67	0.91

Large soil domains were dissected when random perturbations on the stone-soil interface developed into linear stone domains that extended across the soil domain, a process that was particularly active when lateral confinement was only moderate ($C_{sq} < \sim 0.8$, Fig. 3C) or if stone diffusion by lateral squeezing was large relative to lateral sorting ($K_{sq} \gg K_{ls}$). The mean polygon size stabilized when the frequencies of dissection of a soil domain and elimination of a soil domain were similar, generally in the range $\sim 3D_{ls}$ to $\sim 5D_{ls}$.

Sorted polygons in the model and in nature appear similar because of the prevalence of roughly equiangular three-way intersections surrounding nearly equidimensional polygons with a fairly narrow distribution of sizes. As a quantitative test of this model, distributions of intersection angles and normalized polygon areas predicted from the model (using parameters as in Fig. 4) were compared with the corresponding distributions measured from sorted polygon networks within two desiccated pond basins in Alaska (Fig. 5 and Table 1) (*33*). Within the variability between the measured networks, modeled and measured polygons are consistent.

In our model, all forms of sorted patterned ground form via self-organization from just two straightforward feedback mechanisms: lateral sorting and stone domain squeezing. Sharp transitions between patterns occur as three parameters are varied: stone concentration, hillslope gradient, and the relative strength of lateral sorting and squeezing. Squeezing and confinement—which are critical for the development of the most common pattern, sorted polygons—are enhanced by rapid freezing in stone domains with large, air-cooled pores and by low soil compressibility. This model suggests that the presence and type of pattern can be diagnostic of active layer properties and the relative magnitudes of the primary transport processes.

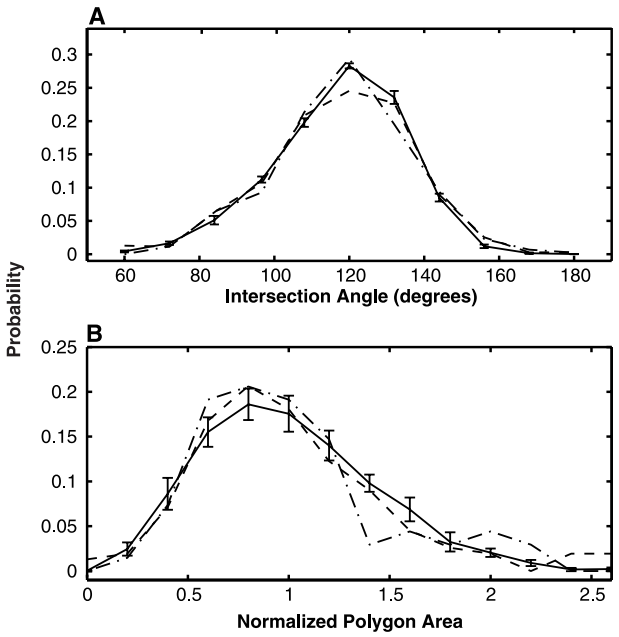

Fig. 5. (**A**) Intersection angle and (**B**) polygon area (normalized by the mean polygon area) probability distributions from sorted polygons in Alaska and predictions from the model using parameters as in Fig. 4, except with simulation size of 30 × 30 m. Dashed line, west pond; dash-dot line, east pond; solid line, model. Error bars represent SD of 10 independent model runs. Model is consistent with measurements within their level of variability.

References and Notes

1. A. L. Washburn, *Geol. Soc. Am. Bull.* **67**, 823 (1956).
2. A. E. Corte, *Biul. Peryglacjalny* **15**, 175 (1966).
3. S. P. Anderson, *Geol. Soc. Am. Bull.* **100**, 609 (1988).
4. S. Taber, *J. Geol.* **37**, 428 (1929).
5. A. C. Fowler, W. B. Krantz, *SIAM J. Appl. Math.* **54**, 1650 (1994).
6. N. Li *et al.*, *Cold Regions Sci. Technol.* **31**, 199 (2000).
7. N. Matsuoka, *Earth Sci. Rev.* **55**, 107 (2001).
8. R. J. Ray *et al.*, *J. Glaciol.* **29**, 317 (1983).
9. K. J. Gleason *et al.*, *Science* **232**, 216 (1986).
10. B. T. Werner, B. Hallet, *Nature* **361**, 142 (1993).
11. M. A. Kessler *et al.*, *J. Geophys. Res.* **106**, 13287 (2001).
12. B. Hallet, *Can. J. Phys.* **68**, 842 (1990).
13. B. T. Werner, T. M. Fink, *Science* **260**, 968 (1993).
14. A. B. Murray, C. Paola, *Nature* **371**, 54 (1994).
15. B. T. Werner, *Geology* **23**, 1107 (1995).
16. H. H. Stolum, *Science* **271**, 1710 (1996).
17. P. Rohani *et al.*, *Trends Ecol. Evol.* **12**, 70 (1997).
18. G. Nicolis, I. Prigogine, *Self-Organization in Nonequilibrium Systems: From Dissipative Structures to Order Through Fluctuations* (Wiley, New York, 1977).
19. J. H. Schmertmann, R. S. Taylor, *Quantitative Data from a Patterned Ground Site over Permafrost* (U.S. Army Cold Regions Research and Engineering Laboratory, Hanover, NH, 1965).
20. F. H. Nicholson, *Arctic Alpine Res.* **8**, 329 (1976).
21. F. A. Cook, *Arctic* **8**, 237 (1955).
22. The lateral sorting feedback is consistent with the limited range of relevant field observations. Frost-susceptible soils overlain by surface stone layers often exhibit lateral sorting associated with soil plugs rising to the surface (*34*). A model for sorted circles based on this lateral sorting feedback is quantitatively consistent with field measurements (*11*).
23. Observations within sorted polygons of upended stones, stones aligned parallel to the stone domain axis, and mud folds parallel to the stone-soil contact are consistent with lateral squeezing of stone domains (*35, 36*).
24. Surface relief across stone domains reflects removal of soil from beneath by frost heave at the stone-soil interface. Because stone domains narrow with depth, frost heave near the ground surface removes soil beneath the edge of the stone domain, whereas frost heave at depth removes soil beneath the center. In steady state, surface gradients are balanced by stone avalanching and removal of soil is balanced by soil addition processes whose impact on elevation is distributed across the stone domain surface.
25. Lateral squeezing is dependent on stone domain width (relative to stone diameter) owing to increased resistance to deformation by narrower stone domains.
26. See supporting data on *Science* Online.
27. Unlike previous simulation models (*10, 11, 37*), stone position is not discretized, avoiding congestion effects that can cause trapping and jamming of stones on lattices. However, here a lattice with grid size corresponding to stone diameter is used to calculate the concentration of stones and to determine the depth to which they are stacked. This semicontinuous algorithm allows for greater sensitivity to local biases because stones can move in any direction and over distances less then a cell width. Stones can also overlap, representing stacking of stones, up to a limit corresponding to the maximum depth of freeze-thaw processes.
28. The length scale D_{ls} corresponds to the maximum lateral distance over which soil is displaced by frost heave (*11*).
29. K_{ls} and K_{sq} are likened to diffusion constants because they quantify the ratio of stone flux to gradient.
30. The magnitude of squeezing depends on the thickness of the ice-rich layer along the near-vertical boundaries between stone and soil domains. Squeezing can be influenced by soil domain size for small soil domains, but well-formed soil domains generally are much larger than the thickness of the ice-rich layer. Therefore, this dependence is not included in the model (i.e., D_{sq} does not depend on soil domain size).
31. D. Weaire, N. Rivier, *Contemp. Phys.* **25**, 59 (1984).
32. F. Elias *et al.*, *Phys. Rev. E* **56**, 3310 (1997).
33. Measured sorted polygons were located in the basins of two desiccated ponds 100 m north of Denali Highway, ~115 km east of Cantwell, Alaska. Both ponds exhibit a gradation from high to low stone concentration moving outward from their centers. Well-formed polygons with narrow stone domains located midway in this gradation were digitized from low-elevation aerial photographs that had been orthorectified using ground control points (*38*). East pond: 68 polygons, 436 angles. West pond: 155 polygons, 705 angles.
34. A. L. Washburn, *Plugs and Plug Circles: A Basic Form of Patterned Ground, Cornwallis Island, Arctic Canada—Origin and Implications* (Geological Society of America, Boulder, CO, 1997).
35. R. P. Goldthwait, *Quat. Res.* **6**, 27 (1976).
36. J. S. Huxley, N. E. Odell, *Geogr. J.* **63**, 207 (1924).
37. F. Ahnert, *Trans. Jpn. Geomorphol. Union* **2**, 301 (1981).
38. Y. I. Abdel-Aziz, H. M. Karara, *Proceedings of the Symposium on Close-Range Photogrammetry* (American Society of Photogrammetry, Falls Church, VA, 1971), pp. 1–18.

39. We thank A. B. Murray and B. Hallet for many helpful discussions, and L. Clarke for assistance in image processing. Supported by NSF Arctic Natural Sciences Program grant OPP-9530860, the Andrew W. Mellon Foundation, a National Defense Science and Engineering Graduate Fellowship, and a student research grant from the Whole Earth Society at Scripps Institution of Oceanography.

Supporting Online Material

www.sciencemag.org/cgi/content/full/299/5605/380/DC1
SOM Text
Fig. S1

13 August 2002; accepted 19 November 2002

The Global Morphology of Wave Poynting Flux: Powering the Aurora

A. Keiling,[1]*† J. R. Wygant,[1] C. A. Cattell,[1] F. S. Mozer,[2] C. T. Russell[3]

Large-scale, electric currents flowing along magnetic field lines into the polar regions of Earth are thought to be the main contributors of the energy that powers the ionospheric aurora. However, we have found evidence for global contributions from electromagnetic waves (Alfvén waves). Data that were collected from the Polar spacecraft over the course of 1 year show that the flow of wave electromagnetic energy at altitudes of 25,000 to 38,000 kilometers delineates the statistical auroral oval. The Poynting flux of individual events distributed along the auroral oval was larger than 5 ergs per square centimeter per second, which is sufficient to power auroral acceleration processes. This evidence suggests that in addition to magnetic field-aligned currents, the dayside and nightside aurora is globally powered by the energy flow of these high-altitude Alfvén waves.

Earth's aurora occurs statistically and often simultaneously in an oval-shaped belt (Fig. 1A) around the magnetic poles (*1*). Magnetic field lines connect this auroral oval to the magnetosphere, the region above the atmosphere that is dominated by Earth's magnetic field and filled